Real-time full-field characterization of soliton dynamics in a microcomb

1st Yuchong Cai
Wuhan National Laboratory for Optoelectronics & School of Optical and Electronic Information, Huazhong University of Science and Technology
Optics Valley Laboratory
Wuhan, China
m202073041@hust.edu.cn

2nd Zichun Liao
Wuhan National Laboratory for Optoelectronics & School of Optical and Electronic Information, Huazhong University of Science and Technology
Optics Valley Laboratory
Wuhan, China
d202281172@hust.edu.cn

3rd Lun Li
Wuhan National Laboratory for Optoelectronics & School of Optical and Electronic Information, Huazhong University of Science and Technology
Optics Valley Laboratory
Wuhan, China
lunli@hust.edu.cn

4th Yaoshuai Li
Wuhan National Laboratory for Optoelectronics & School of Optical and Electronic Information, Huazhong University of Science and Technology
Optics Valley Laboratory
Wuhan, China
liyaoshuai@hust.edu.cn

5th Chi Zhang*
Wuhan National Laboratory for Optoelectronics & School of Optical and Electronic Information, Huazhong University of Science and Technology
Optics Valley Laboratory
Wuhan, China
chizheung@hust.edu.cn

6th Xinliang Zhang
Wuhan National Laboratory for Optoelectronics & School of Optical and Electronic Information, Huazhong University of Science and Technology
Optics Valley Laboratory
Wuhan, China
xlzhang@mail.hust.edu.cn

***Abstract*—Real-time full-field characterization of the process of soliton number switching is realized by the chirped coherent detection system, with a temporal resolution of 0.3ps, and a time recording length of 550 ps.**

Keywords—*microcomb, soliton dynamics, coherent detection, optical Fourier transform*

I. Introduction

Since the first microresonator-based frequency comb (microcombs) was realized by Del'Haye in 2007 [1], considerable progress has been made in microcombs generation in the last ten years and nowadays microcombs are widely applied in various fields such as metrology [2], microwave photonics [3], optical communication [4] and present unprecedented performances. Meanwhile, there are many interesting soliton phenomena in microcombs such as turning rolls [5], dark pulses [6], soliton crystals [7], dispersive waves [8]. For the further improvement of the dynamics of the solitons in microcombs and expand the applications, the real-time characterization of the solitons in microcombs is very necessary.

Due to ultrahigh-quality factor (Q) of the microresonators, the transition dynamics evolution is much longer than the cavity roundtrip in the time-domain, which causes great challenges in real-time observation. In the past few years, a lot of researches focusing on how to capture the soliton dynamics in microresonators have been published [9,10]. The methods of observing the transition mainly include ultrafast temporal magnifier and optical sampling. Either of them offers an opportunity to capture the soliton dynamics accurately which is a very useful tool for studying the microresonator physics. However, due to the ultrahigh free-spectral-range (FSR) of the microresonators, as for real-time spectral characterization of soliton dynamics in microresonators, which can provide a comprehensive perspective in soliton dynamics, there is still no an ideal way.

In this paper, based on optical Fourier transform and coherent detection, the real-time full-field spectral and temporal characterization of the process of soliton number switching is realized, for the first time, with about 25-nm bandwidth and 0.3-ps temporal resolution, as well as a high measurement speed of ~20 MHz. The soliton signal is generated by a resonator with a FSR of ~48.97 GHz and intrinsic Q factor of above 2 million. As a proof-of-concept, the system is used to observe the dissipative Kerr soliton transition dynamics during the pump laser scanning. It can provide a useful tool for developing new soliton applications and understanding the complex soliton dynamics much better in microcavities.

II. Experiment Description

The experimental setup for the characterization of the full-field soliton dynamics transition in a microcomb is shown in Figure 1(a), which consists of solitons with reference and chirped coherent detection. A mode-locked fiber laser (MLFL) with an FSR of about 20 MHz is used for the local oscillator (LO), propagating through a dispersion compensation fiber (DCF), whose dispersion is about 2120 ps^2, mapped into the frequency-mapped waveform. To avoid the stretched pulse train aliasing, a band-pass-filter, from 1540 to 1565 nm is used. The transmission spectrum of the filtered LO (red curve) and the stretched temporal waveform (blue curve) are shown in Figure 1(b). The experimental setup of soliton generation is shown in Figure 1(c). By using an auxiliary laser that passively stabilizes intracavity power, we could stably and efficiently generate solitons in the Hydex microresonator. The tuning rate of the pump frequency can be significantly reduced under the thermal compensation of auxiliary laser, and the pump frequency can be tuned manually to generate soliton states stably. The transmission spectrum of the microresonator near the auxiliary laser can be monitored by a vector network analyzer (VNA). The VNA has two main functions. One is to optimize the polarization state of the auxiliary light. The other is to monitor the detuning of the auxiliary and adjacent resonant peak in real-time optimizing the degree of the auxiliary thermal compensation.

In this work, the power of the auxiliary laser is about 2 W, and we adjust the polarization of the auxiliary laser which makes the microcomb in the over-compensated state [11,12]. Under this condition, the thermal effect is mainly controlled by the auxiliary laser intracavity power. During the forward

National Key Research and Development Program of China (Grant Nos. 2022YFF0705904) and the National Natural Science Foundation of China (Grant Nos. 62075072, and 61927817).

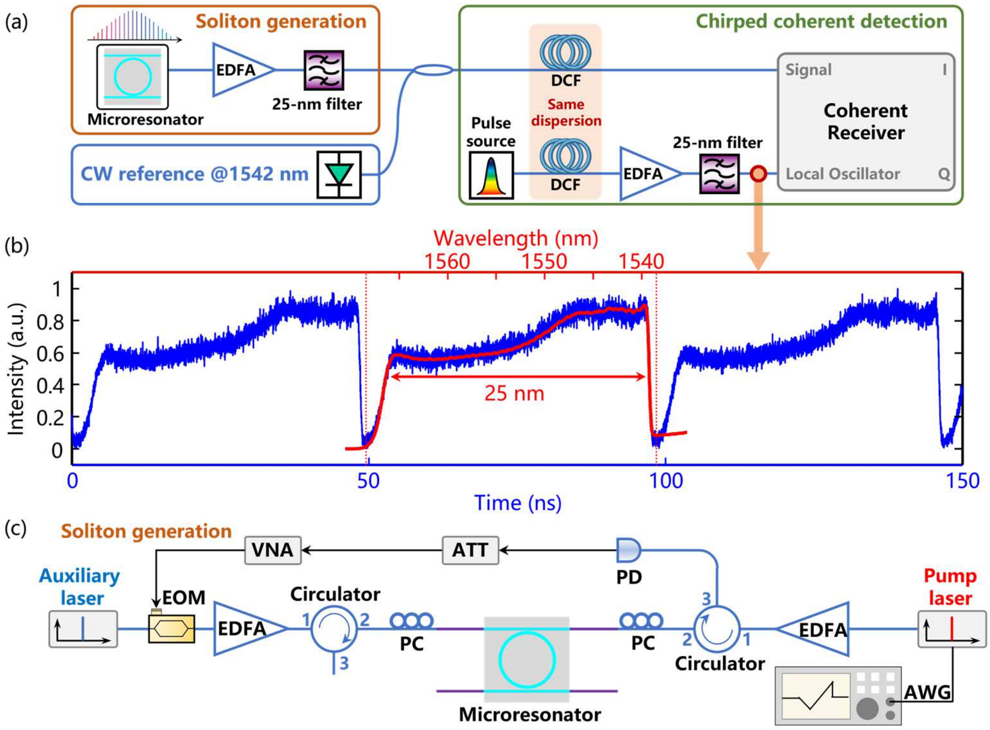

Fig. 1. The schematic diagram of the observation system in the experiment. (a) Experimental setup of the observation system. (b) The spectrum (red curve) and the stretched temporal waveform (blue curve) of the filtered pulse. (c) Experimental setup of soliton generation.

tuning processes of the pump laser, because of the pump Q-power product weaker than the auxiliary Q-power product variation, the intracavity power increases leading to the resonant peak red-shifts and soliton numbers decreasing. Besides, under the over-compensated state, during the backward tuning processes, the soliton numbers increase. In order to achieve the soliton numbers switching, firstly, we adjusted the TEC to make the pump laser enter the red-shift detuning region of the resonant peak. Then the soliton number switching is achieved by using an arbitrary waveform generator (AWG) to adjust the pump wavelength.

The signal under test (SUT) generated by a microcomb, through a DCF whose dispersion is nearly equal to the DCF of the LO is optical Fourier transformed to the temporal spectrum with the same wavelength-to-time relationship. Then, through the fiber Bragg grating (FBG), the pump laser at 1553 nm and the auxiliary laser at 1550 nm are both filtered out to suppress the pump and the auxiliary power which otherwise saturates the coherent receiver. Meanwhile, to determine the detected spectrum of the SUT, a continuous-wave (CW) laser at 1542 nm is used as the reference wavelength, which is filtered out in the subsequent digital signal process (DSP). Then the frequency-mapped SUT and the reference CW are both sent to the signal port of the coherent receiver with a bandwidth of ~25 GHz. Another port of the coherent receiver is connected to the stretched LO with the same wavelength-to-time relationship, so that the hybrid frequency is always at the fundamental frequency within the bandwidth of the used coherent receiver. Therefore, the detection bandwidth of the proposed system is equal to the filtered LO of ~25 nm, that is to say the temporal resolution of ~300 fs. At a frame rate of ~20 MHz for the system and with a 550-ps single-shot recording length, we could successfully measure the full-field intracavity temporal waveform of 27 roundtrips in one shot; however, miss the information between every frame. Then, multiple frames are stitched to reconstruct the soliton dynamic transition. As long as the soliton dynamics evolution is much slower than the system frame rate, the system can capture valuable information about the soliton dynamics transition.

III. Results and Discussion

To prove the capability of the proposed system, firstly, we measured a stable four-soliton state shown in Figure 2. As shown in Figure 2(a), the spectrum of a stable singlet soliton state is detected by the proposed system (blue curve) with a bandwidth of ~25 nm, limited by the bandwidth of the LO, which fits well with the result detected by an optical spectrum analyzer (OSA) (red curve), showing outstanding ability of obtaining spectrum. Figure 2(b) shows one frame of the detected waveform and the blue curve is the measured temporal intensity while the red curve is the measured temporal phase. The time recording length of the system is about 550 ps, determined by the bandwidth of the coherent receiver and the dispersion of the DCF. Figure 2(c) is a zoom-in version of Fig. 2(b) from 20 to 60 ps, which consists of two periods for the microcomb. From the temporal intensity (red curve), it is clear that there are four solitons in the microcavity. The temporal phase (blue curve) is flat in the duration of the pulses.

The result of a stable four-soliton state indicates that the proposed system could characterize both the real-time full-field temporal soliton dynamics and real-time spectrum. As mentioned above, by using an auxiliary laser, the process of the microcomb soliton number switching is in the over-compensated states. Then, by adjusting the wavelength of the pump laser, under pump power of 2 W, the soliton dynamics transition in the over-compensated state, is shown in Figure 3. We mainly focus on the soliton dynamics transition during the pump laser forward tuning processing. The comb power is

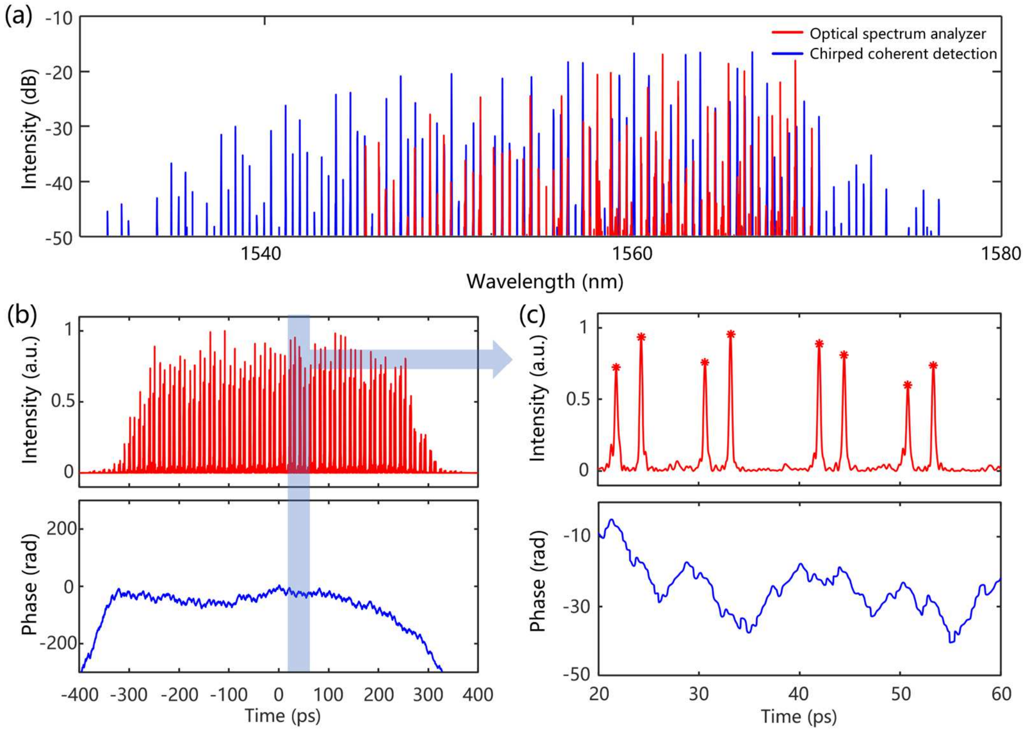

Fig. 2. Observing a stable four-soliton state with the proposed system. (a) The spectrum of a stable singlet soliton state detected by an OSA (red curve) and the chirped coherent detection (blue curve). (b) A frame of a stable soliton singlet soliton state observed by the proposed system. The blue curve is the intensity of the temporal waveform and the red curve is the phase of the temporal waveform. (c) The zoom-in version of (b), indicating a four-soliton state.

recorded by a photodetector with a bandwidth of 125 MHz, which is shown in Figure 3(a), during the forward tuning processes of the pump laser with the power of 2 W. As the pump laser is away from the resonant peak, a stable multiple soliton state is gradually stabilized. With further forward turning, the intensity of the microcomb are decreasing and the intracavity solitons are successively extinct, finally, reaching the singlet soliton state. Meanwhile, the process of the soliton dynamics was observed in real time based the chirped coherent detection system. Figure 3(b) is the 2D temporal evolution of Figure 3(a) from 34 to 44 μs, depicting the soliton numbers switching. Within this time range, there are four soliton states, respectively, the five-soliton state, the four-soliton state, the three-soliton state and the singlet soliton

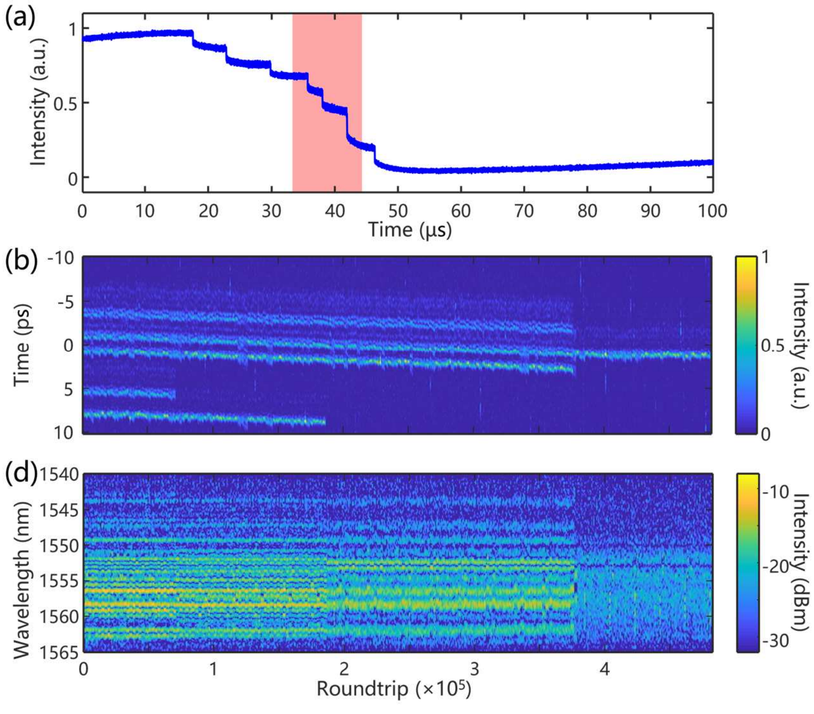

Fig. 3. Observing a stable four-soliton state with the proposed system. (a) The experimental trace of the output microcomb when the pump laser is tuned forward across a few soliton states. (b) The 2D evolution portrait of the red area in (a), depicting soliton numbers switching from a five-soliton state to a singlet soliton state. (c) The 2D evolution of the spectrum of the single roundtrip.

state. The intensity decreasing in Figure 3(a) corresponds to the process of soliton number switching in Figure 3(b). While, the real-time spectral soliton dynamics is shown in Figure 3(c), indicating a good correspondence to Figure 3(b).

IV. CONCLUSIONS

In summary, by using an auxiliary laser, the microcavity could stably and efficiently generate solitons. The observations of a stable four-soliton state have proved the system ability of capturing the real-time temporal full-field waveforms. We mainly observed the soliton numbers switching in the over-compensated states during the pump laser forward tuning processing. It is difficult to observe the spectral evolution of the microcomb solitons. Here, the characterization of the temporal full-field soliton dynamics transition has been realized by the chirped coherent detection system as well as the real-time spectrum, with a time resolution of 0.3 ps, and a time recording length of 550 ps, which results in a time-bandwidth product (TBWP) of ~1800. The results of the characterization of the soliton number switching process clearly shows the intracavity solitons motor process. It could become a useful tool for the understanding of complex soliton physics and developing new microcomb soliton applications.

ACKNOWLEDGMENT

This work was supported by grants from the National Key Research and Development Program of China (Grant Nos. 2022YFF0705904) and the National Natural Science Foundation of China (Grant Nos. 62075072, and 61927817).

REFERENCES

[1] P. Del'Haye, A. Schliesser, O. Arcizet, T. Wilken, R. Holzwarth and T. J. Kippenberg, "Optical frequency comb generation from a monolithic microresonator," Nature **450**, 1214–1217 (2007).

[2] P. Trocha, et al, "Ultrafast optical ranging using microresonator soliton frequency combs," Science, **359**, 887-891 (2018).

[3] W. Liang, et al, "High spectral purity Kerr frequency comb radio frequency photonic oscillator," Nat. Commun. **6**, 7957 (2015).

[4] P. Marin-Palomo, et al, "Microresonator-based solitons for massively parallel coherent optical communications," Nature **546**, 274-279 (2017).

[5] Z. Qi, S. Wang, et al, "Dissipative cnoidal waves (Turing rolls) and the soliton limit in microring resonators, " Optica **6**, 1220-1232 (2019).

[6] E. Nazemosadat, et al, "Switching dynamics of dark-pulse Kerr frequency comb states in optical microresonators," Phys. Rev. A **103**, 013513, (2021).

[7] D. C. Cole, E. S. Lamb, P. Del'Haye, S. A. Diddams, and S. B. Papp, "Soliton crystals in Kerr resonators," Nat. Photon. **11**, 671-676 (2017).

[8] Q.-F. Yang, X. Yi, K. Y. Yang, and K. Vahala, "Spatial-mode-interaction-induced dispersive waves and their active tuning in microresonators," Optica **3**, 1132-1135 (2016).

[9] B. Li, S. Huang, Y. Li, C. Wong, and K. K. Wong, "Panoramic-reconstruction temporal imaging for seamless measurements of slowly-evolved femtosecond pulse dynamics,“ Nat. Commun. **8**, 1-10 (2017).

[10] X. Yi, Q. Yang, K. Yang, and K. Vahala, "Imaging soliton dynamics in optical microcavities," Nat. Commun. **9**, 3565 (2018).

[11] S. Zhang, et al, "Sub-milliwatt-level microresonator solitons with extended access range using an auxiliary laser," Optica **6**, 206-212 (2019).

[12] Y. Zhao, et al, "Soliton Burst and Bi-Directional Switching in the Platform with Positive Thermal-Refractive Coefficient Using an Auxiliary Laser," Laser & Photonics Reviews, **15**, 2100264 (2021).